

Numerical Simulations of Type Ia Supernova Explosions

F.K. Röpkel¹, W. Hillebrandt¹, M. Gieseler¹, M. Reinecke¹, and C. Travaglio²

¹ *Max-Planck-Institut für Astrophysik, Karl-Schwarzschild-Str. 1, 85741 Garching, Germany*

² *INAF – Osservatorio Astronomico di Torino, Strada dell'Osservatorio 20, I-10025 Pino Torinese, Torino, Italy*

1.1 Introduction

Recent numerical simulations of Type Ia Supernova (SN Ia) explosions [1, 2] have successfully modeled the Chandrasekhar-mass deflagration scenario (for a review see [3] or J. Niemeyer's contribution to these proceedings) in three spatial dimensions. In this SN Ia model a carbon/oxygen white dwarf (WD) star accretes matter from a binary companion until it reaches the Chandrasekhar mass. At this point, thermonuclear burning in the center of the WD forms a subsonic deflagration flame which—mediated by thermal conduction of the degenerate electrons—propagates outward. Since the resulting stratification of dense fuel and light ashes in the gravitational field is unstable (Rayleigh-Taylor instability), burning bubbles of hot ashes ascend into cold fuel. At the interfaces a secondary shear instability gives rise to the local development of turbulence which wrinkles the flame front. This effect accelerates the effective burning velocity and thus the energy generation can account for SN Ia explosions. In the explosion process the WD material is converted to iron group elements and a smaller fraction of intermediate-mass elements (like Si, S, and Ca). However, it is only the radioactive decay of ⁵⁶Ni that powers the observed lightcurve.

Numerical implementations of such models must fulfill a number of requirements. They have to be robust against variations of the initial conditions in an astrophysically reasonable range, but on the other hand they are expected to explain the observed diversity of SNe Ia. The final goal is, of course, to explain the correlation between the peak luminosity and the light curve shape on the basis of theoretical models. This relation is of great importance to calibrate cosmological distance measurements. Three-dimensional SN Ia explosion simulations have reached a quality where these issues can be addressed. Furthermore, nucleosynthetic post-processing of the explosion data has opened the possibility to calculate synthetic light curves and spectra which can be directly compared to observations. This provides a way to discriminate between different astrophysical models (e.g. pure deflagration or delayed detonation).

We present the first systematic study on what answers three-dimensional deflagration models can give. What are the possible parameters that have the potential to explain the SN Ia diversity? Among others the progenitor's carbon-to-oxygen ratio, its metallicity, and the central density at ignition are commonly suggested. In our survey we vary these three parameters independently to explore the effects on the explosion models. However, we are aware of the fact that in principle they are interrelated by stellar evolution of the progenitor WD star. Our study covers the following parameter space: We apply three different carbon mass fractions of the WD material, $X(^{12}\text{C}) = 0.30, 0.46, 0.62$, three different central densities

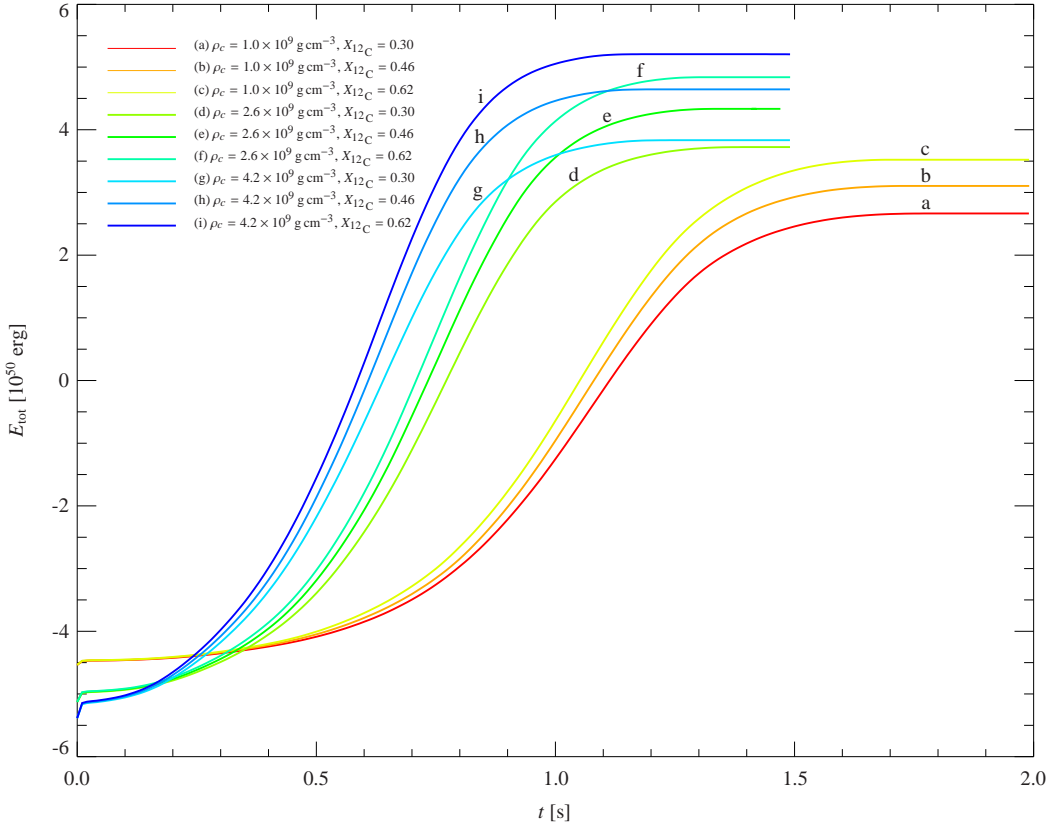


Figure 1: Total energy of the different models as a function of time.

at ignition, $\rho_c = [1.0, 2.6, 4.2] \times 10^9 \text{ g cm}^{-3}$, and three different metallicities of the WD (represented by the ^{22}Ne mass fraction), $Z = [0.3, 1.0, 3.0]Z_\odot$. This defines the 27 models of our survey.

1.2 Numerical models

Our numerical model is based on the PROMETHEUS implementation [4] and describes the flame as a discontinuity between fuel and ashes applying the level set method [5]. Turbulence on unresolved scales is treated with a subgrid-scale model [6]. Details of the implementation can be found in [7, 8]. The thermonuclear burning is assumed to proceed to nuclear statistical equilibrium (NSE) consisting of iron group elements (represented by “Ni” in our model) and α -particles at high fuel densities. Below $\rho_{\text{fuel}} = 5.25 \times 10^7 \text{ g cm}^{-3}$ burning is assumed to terminate at intermediate mass elements represented by “Mg” and below $\rho_{\text{fuel}} = 1.0 \times 10^7 \text{ g cm}^{-3}$ the reactions are so slow that it is no longer followed. Our numerical setup is analogous to the *c3-3d-256* model of [8]. The carbon/oxygen ratio of the progenitor and the central density at ignition are varied in the explosion models. In these models tracer particles are distributed equally in mass shells. They record the temperature, the density, and the internal energy of the explosion process. With help of this data it is possible to post-process the nucleosynthesis of the explosion models (see C. Travaglio’s contribution to these proceedings). Here the WD’s metallicity is varied by changing the mass fraction of ^{22}Ne .

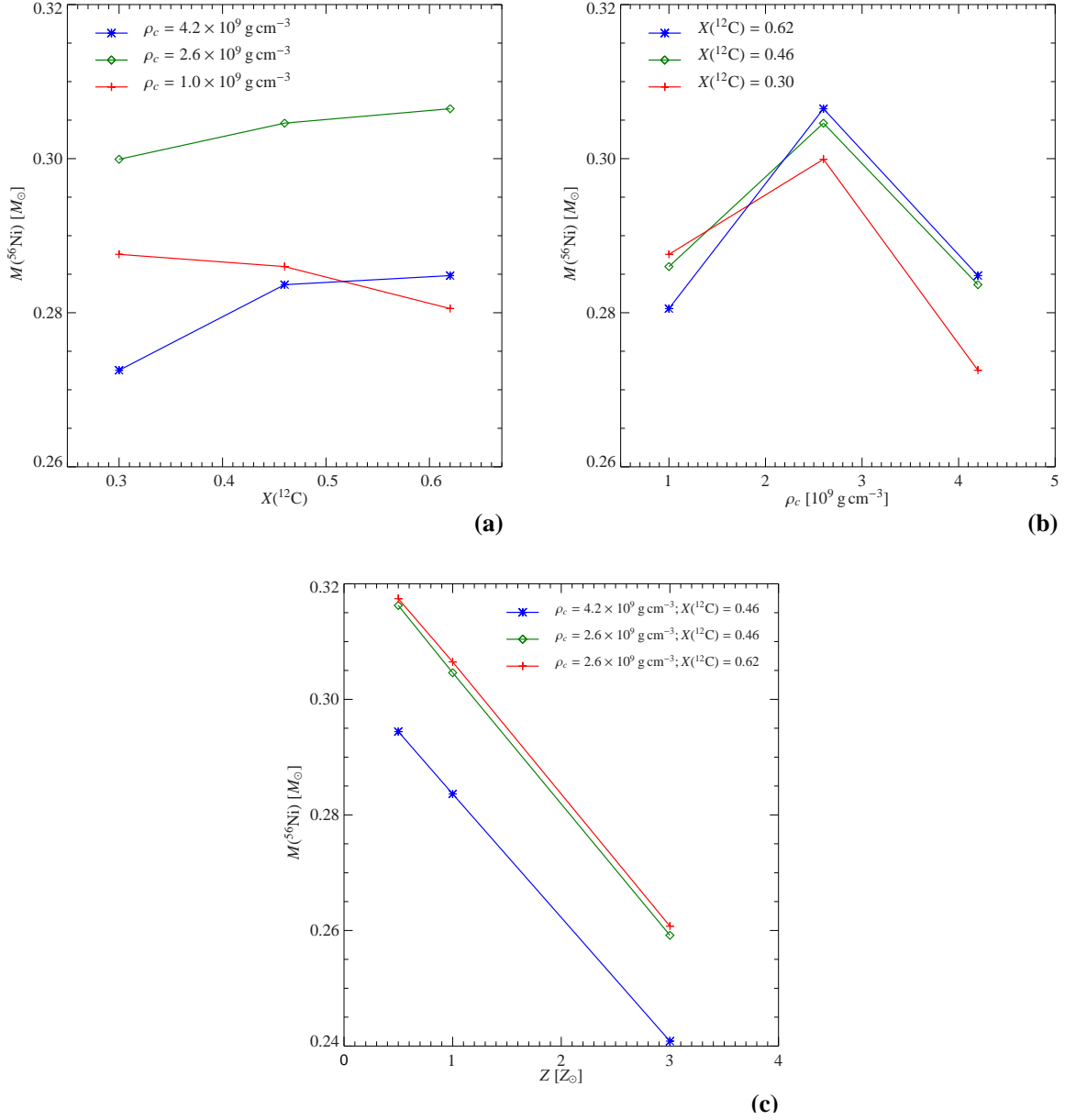


Figure 2: ^{56}Ni masses produced by the models as a function of (a) carbon mass fraction of the progenitor, (b) central density at ignition, and (c) progenitor's metallicity .

1.3 Results

Figure 1 shows the total energy of our models. Obviously, a lower central density leads to a lower energy release and delays the evolution of the model. The differences in the total energy productions for varying ρ_c and fixed other parameters amount to $\sim 40\%$. The reason for this effect is the different gravitational acceleration experienced the flame front which leads to a change in the evolution of the nonlinear Rayleigh-Taylor instabilities. For higher ρ_c the evolution is faster and more pronounced, so that the flame is affected by stronger turbulence.

This accelerates the flame propagation and leads to an increased energy release.

Contrary to that, a change in the carbon mass fraction does not lead to a significant delay of the evolution. The change of the total energy production of the models amounts to $\sim 12\%$. This is due to the different binding energies of fuel with varying C/O ratio.

The ^{56}Ni masses produced by the different models are plotted in Fig. 2. With increasing central density of the WD at ignition, the ^{56}Ni production rises to a maximum at $\rho_c \approx 2.5 \times 10^9 \text{ g cm}^{-3}$ and then declines again (cf. Fig. 2b). The variation is of the order of 10%. This behavior can be expected from the fact that two effects are competing here. The effect of the different gravitational acceleration experienced by the flame leads to a faster flame propagation for higher ρ_c , as discussed above. Consequently, more material is processed at high densities resulting in an increased amount of iron group elements. On the other hand, at higher densities the neutronization of the burnt material becomes important and thus an increasing fraction of the iron group elements is present in form of neutron-rich nuclei (like ^{58}Ni) instead of ^{56}Ni .

With increasing metallicity of the progenitor, i.e. higher mass fraction of ^{22}Ne (a nucleus with neutron excess), neutron-rich iron group nuclei in the ashes are favored and less ^{56}Ni is produced. This is evident in our models (cf. Fig. 2c). The variation amounts to $\sim 20\%$. Our results are consistent with a linear relation that was proposed by [9] (see also the contribution of E. Brown to these proceedings).

With varying $X(^{12}\text{C})$ the change in the nickel masses is only of the order of a few percent (see Fig. 2a). This result is unexpected in a simple picture. Although the total explosion energy increases with $X(^{12}\text{C})$, the flame evolution in the different models is found to be surprisingly similar. This results in little changes in the ^{56}Ni production. The explanation of this effect is a higher fraction of α -particles in NSE in the ashes at maximum energy generation for increasing $X(^{12}\text{C})$. This acts as an energy buffer due to the reduction of the binding energy and increased particle number in the burnt material. Details can be found in [10].

1.4 Conclusions

In the present study it has been shown that our SN Ia models are robust to astrophysically reasonable variations in the initial parameters. To what degree the deflagration scenario is able to explain the full observed SN Ia sample has to be decided by more detailed studies. The current survey indicates that it can account for some of the observed features. A simple deduction of the peak luminosities from the ^{56}Ni masses (Arnett’s rule, [11]) produced by our models leads a diversity in the luminosities that can—at least partly—explain the observed scatter.

However, it would predict a significant change with varying metallicity but almost no change with varying C/O ratio of the progenitor WD. On the other hand, the former will not influence the explosion dynamics while the latter leads to a significant change in the total energy release. Thus the light curve shape will probably not change much in the first case but vary significantly in the second. Therefore, it is clear that a single parameter will not explain the peak luminosity–light curve shape relation of SNe Ia. It seems likely that a combination of progenitor parameters (based on stellar evolution models of the WD) will be necessary for this task. Additionally, synthetic light curves from the models are needed to deduce their characteristics and to take into account multidimensional effects. Arnett’s rule may be a too strong simplification here. One of the next steps in improving the explosion models will be a

refined description of the thermonuclear reactions. Moreover, it will be necessary to take into account electron captures at high densities to improve the reliability of the results for varying central densities at ignition. A detailed analysis of the parameter study presented here can be found in [12].

Acknowledgements

The junior authors of this text would like to congratulate W. Hillebrandt on his 60th birthday.

References

- [1] M. Reinecke, W. Hillebrandt, and J.C. Niemeyer, *A&A* **391** (2002) 1167.
- [2] V.N. Gamezo, A.M. Khokhlov, E.S. Oran, A.Y. Chtchelkanova, and R.O. Rosenberg, *Science* **299** (2003) 77.
- [3] W. Hillebrandt and J.C. Niemeyer, *Annu. Rev. Astron. Astrophys.* **38** (2000) 191.
- [4] B.A. Fryxell and E. Müller, MPA Green Report **449** (Max-Planck-Institut für Astrophysik, Garching, 1989).
- [5] S. Osher and J.A. Sethian, *J. Comp. Phys.* **79** (1988) 12.
- [6] J.C. Niemeyer and W. Hillebrandt, *ApJ* **452** (1995) 769.
- [7] M. Reinecke, W. Hillebrandt, J.C. Niemeyer, R. Klein, and A. Gröbl, *A&A* **347** (1999) 724.
- [8] M. Reinecke, W. Hillebrandt, and J.C. Niemeyer, *A&A* **386** (2002) 936.
- [9] F.X. Timmes, E.F. Brown, and J.W. Truran, *ApJ* **590** (2002) L83.
- [10] F.K. Röpke and W. Hillebrandt, *A&A Lett.* (2004) in press.
- [11] W.D. Arnett, *ApJ* **253** (1982) 785.
- [12] F.K. Röpke, M. Gieseler, M. Reinecke, C. Travaglio, and W. Hillebrandt, (2004) in preparation.